Covalent Functionalization of Few-Layer Black Phosphorus using Iodonium Salts and Comparison to Diazonium Modified Black Phosphorus

Maart van Druenen[1, 2], Fionán Davitt[1, 2], Timothy Collins[1], Colm Glynn[1], Colm O'Dwyer[1] Justin D. Holmes[1, 2] and Gillian Collins[*1, 2]

[1]*School of Chemistry & Tyndall National Institute, University College Cork, Cork, T12 YN60, Ireland.*

[2]*CRANN@AMBER, Trinity College Dublin, Dublin 2, Ireland.*

Abstract

Since the isolation of two dimensional (2D) phosphorene, black phosphorus (BP) has gained popularity due to its high carrier mobility and tunable bandgap. Poor ambient stability of BP remains a key issue and impedes its use in electronic applications. Here we report a new stabilization strategy based on covalent functionalization of liquid exfoliated few-layer BP using aryl iodonium salts. Arylation of BP using iodonium salts enables covalent modification without inducing oxidation and alters the degradation chemistry of BP by inhibiting bridged oxygen formation through attachment to surface oxygen sites. In comparison, functionalization using aryl diazonium salts results in oxidation, aryl multilayer formation and does not adequately disrupt non-covalent solvent passivation. Aryl functionalization of BP using iodonium salts displays superior ambient stability compared to arylation using diazonium salts associated with greater covalent functionalization as characterized using x-ray photoelectron spectroscopy, scanning transmission electron microscopy, photoluminescence and attenuated total reflectance infrared spectroscopy.

Introduction

BP is a semiconductor that displays a high carrier mobility and direct band gap in mono- and few layer[1] form making it an attractive candidate for electronic applications.[2–5] Its layered

structure allows exfoliation of few-layer flakes through mechanical exfoliation which is used for the production of many 2D materials, however, scalability of this process is limited.[2] Liquid exfoliation[6–8] has recently been reported to produce exfoliated BP with increased ambient stability due to the protection of a solvation shell, allowing for easier processing and scalability.[9] Due to the ambient instability of BP, capping layers such as boron nitride or Al_xO_y have been deposited on the surface to prevent degradation and preserve high carrier mobilities in BP FETs.[10,11] Ion doping using sulfur[12] or tellurium[13] has been used to influence the electrical properties of BP and increase its ambient stability assessed using AFM analysis. Furthermore, hybrid aerogels prepared using graphene oxide were found to increase the photothermal stability.[14] BP graphite composites prepared by ball milling produced P-C bonds leading to high performance battery anodes.[15] Covalent functionalization of BP with a conjugated polymer increased stability and improves solubility in organic solvents favorable for fabrication of electronic devices by using traditional spin-coating.[16] Chemical functionalization methods can passivate BP through covalent or non-covalent interactions[17–19] and was first reported by Ryder *et al.*[17] where covalent functionalization of mechanically exfoliated BP using diazonium salts increased the stability of BP. An advantage of this chemical functionalization is the potential to influence the electronic properties of BP due to attachment of various aryl groups with different electron withdrawing substituents. However, the surface chemistry of diazonium functionalized BP was not studied in detail. Abellán *et al.*[18] used non-covalent functionalization of bulk BP with 7,7,8,8-tetracyano-*p*-quinodimethane to improve ambient stability and facilitate electron transfer from BP. Sofer *et al.*[19] reported that diazonium salts, Grignard and alkyl lithium reagents were rather ineffective or led to oxidation of liquid exfoliated BP. They found species that undergo nucleophilic substitution reactions with either P or surface oxygen sites to be highly effective for surface functionalization, although stability was not assessed. The nature of few-layer BP

means its surface chemistry is relatively unexplored but the prospect of functionalizing both P and O surface functionalities opens up a multitude of possible covalent functionalization routes. A critical challenge observed in wet chemical functionalization methods is further oxidation of BP under the reaction conditions. Diaryliodonium salts are a powerful tool in organic synthesis being capable of smoothly arylating nucleophiles under mild conditions.[20–22] Their highly electron deficient nature and the excellent leaving-group ability of aryl iodides make them versatile arylating agents used for arylation of organophosphorus species[23–25] thus a promising candidate for BP modification. Covalent functionalization has not yet been reported on liquid exfoliated, highly monolayer-enriched BP. In this article, we demonstrate a new method for covalent functionalization of liquid exfoliated BP using aryliodonium salts. Iodonium salts have been used for electrochemical functionalization of carbon electrodes,[26] carbon nanotubes (CNTs)[27] and graphene,[28] where increased control can be achieved due to their lower reactivity when compared to diazonium salts.[28,29] Wet chemical functionalization of carbon surfaces with iodonium salts was reported by He *et al*.[27] using sodium naphthalide for reductive activation of graphite and CNTs. Here we demonstrate that iodonium salts react spontaneously with liquid exfoliated few layer BP at room temperature resulting in aryl functionalized surfaces. Covalent modification of BP significantly enhances its ambient stability compared to bare BP. We further demonstrate that functionalization using iodonium and diazonium salts yield different surface modifications. Aryliodonium salts produce aryl-modified BP with superior oxidation resistance, while diazonium salts produce mixed covalent and non-covalent functionalization with the presence of aryl multilayers.

Experimental Section

Materials

Black phosphorus (BP) was purchased from Smart Elements (purity 99.998 %) and all chemicals were purchased from Sigma- Aldrich. Anhydrous N-methyl pyrrolidone (NMP) and acetonitrile (ACN) were stored in a glovebox and transfer of solvents and precursors was carried out in a glovebox while purification after functionalization reactions and centrifugation steps were carried out in ambient conditions.

Exfoliation and Functionalization

Anhydrous NMP and ACN were degassed using at least 7 freeze-pump-thaw cycles and subsequently purged using Ar gas for 1 h. BP was exfoliated in NMP in a Schlenk flask submersed in a bath sonicator (Branson 1800) under a constant flow of Ar for ~20 h. After exfoliation, the solution was left to settle overnight and subsequently centrifuged at 2000 rpm for 30 min. The sediment was discarded to exclude unexfoliated material. The supernatant was centrifuged at 14500 rpm for 40 min to obtain an exfoliated BP sample. The BP was functionalized using a 10 mM solution of methoxybenzenediazonium tetrafluoroborate (MBD), 3,5-bis(trifluoromethyl)benzenediazonium tetrafluoroborate (FBD), 4-nitrobenzenediazonium tetrafluoroborate (NBD), bis(4-fluorophenyl)iodonium triflate (FPI), (perfluoro-n-propyl)phenyliodonium triflate (PPI) or bis(4-methylphenyl)iodonium hexfluorophosphate (MPI) and 100 mM tetrabutylammonium hexafluorophosphate in ACN for 3 h under flow of Ar. Iodonium precursor solutions were dried over molecular sieves for 24 h prior to functionalization. Optimization of reaction parameters using FPI was carried out by (i) increasing the reaction time to 24 h and (ii) heating the reaction mixture to 45 °C. After functionalization the BP was purified using 3 washes with ACN. The concentrated solution was drop cast onto a Si wafer or Si coated in a Ti layer to minimize Si contributions during the XPS analysis.

Characterization

X-Ray photoelectron spectroscopy (XPS) analysis was carried out on an Oxford Applied Research Escabase XPS system with a nonmonochromated Al Kα X-Ray source at 200 W with a base pressure of 5 x 10^{-10} mbar. Survey spectra were acquired at 0-1000 eV using a step size of 0.7 eV, a dwell time of 0.3 s and a pass energy of 50 eV. Core level scans were averaged over 20-40 scans at a step size of 0.1 eV, a dwell time of 0.1 s and a pass energy of 20 eV. CasaXPS software was used to process the spectra with Shirley background correction and peaks fitted to Voigt profiles. Peaks were charge corrected to the C 1s peak at 285 eV. Attenuated total reflectance infrared (ATR-IR) spectra were recorded using a Nicolet 6700 Infrared Spectrometer with a VariGATR, a liquid cooled MgCdTe detector and Smart ITR accessory. Spectra were collected under ambient atmosphere and averaged over 300 scans at a resolution of 2 cm^{-1}. Raman scattering spectra were acquired using a QE65PRO OceanOptics spectrometer with a 50 μm width slit coupled to a microscope with a 40× objective for focusing on the surface of substrates. A Laser Quantum GEM DPSS 532 nm laser was used for excitation. Photoluminescence spectroscopy was used to probe the electronic structure of the samples. Testing was carried out at room temperature using a 532 nm Laser Quantum GEM DPSSexcitation source. Photoluminescence spectra were recorded using a Horiba iHR320spectrometer equipped with a thermoelectrically cooled Syncerity CCD matrix. Scanning transmission electron microscopy (STEM) and Scanning electron microscopy (SEM) analysis was undertaken on an FEI Helios NanoLab 600i scanning electron microscope operating at 20 kV. Transmission electron microscopy (TEM) analysis was acquired on a Jeol 2100 at an operating accelerating voltage of 200 kV. UV analysis was carried out on a Thermo Scientific Evolution 60 S UV-Visible spectrophotometer with a resolution of ±0.8 nm using a Xenon light source in the 200-1100 nm range. The surface topography of the flakes was imaged using atomic force microscopy (AFM, Park Systems XE-100) following drop casting onto a Si substrate. Scans were performed in non-contact

mode under ambient conditions using a non-contact cantilever with a high resolution super sharp tip (SSS-NCHR).

Results and Discussion

BP was exfoliated using liquid exfoliation in NMP under inert conditions (see experimental section). [8,30] TEM analysis shown in Figure 1a and Figure S1 (see Supporting Information) shows a d-spacing of 0.33 nm corresponding to the (010) plane of BP and indicates no damage was induced during the exfoliation process. Additional SEM and STEM analysis of bare BP is shown in Figure S2 (a)-(c). UV analysis in Figure S3 displays the absorption spectrum of BP in agreement with previously reported UV spectra.[8,31] Figure 1b displays the P 2p XPS peak of exfoliated BP showing the P-P bonds at a binding energy (B. E.) of 130 eV and oxide associated peaks in the range of 132-135 eV. Exfoliated BP typically displays a 15-20 % oxide shoulder with respect to the elemental P 2p peak which is consistent with literature.[8] After functionalization with bis(4-fluorophenyl)iodonium triflate (FPI) the P 2p core level showed no increase in oxidation during the reaction. In comparison, functionalization using diazonium salts induced BP oxidation, which increased the oxide shoulder from 20 % to ~30 % (Figure S4). The formation of a second phosphorous oxide environment for diazonium modified BP can be attributed to phosphorus in a higher oxidation state as shown in the P 2p core levels which is indicative of significant oxidation of the BP surface.[32,33] The survey spectra of bare and FPI functionalized BP are displayed in Figure S5. The presence of the F 1s and absence of the I 3d peak indicates reaction of the iodonium moiety resulting in attachment of F-Ar groups. AFM analysis of the liquid exfoliated BP displayed in Figure 1e and g shows a height profile of 17 nm indicating exfoliation produced few-layer flakes. AFM analysis after functionalization shown in Figure 1f indicate the flakes maintain well-defined edges and do not undergo degradation during functionalization. Figure 1c shows Raman spectra of exfoliated and aryl functionalized BP.

The A^1_g, B^2_g and A^2_g phonon modes of BP located at 367, 444 and 472 cm^{-1}, are in agreement with the literature[8] and indicate no damage occurred to the BP crystal structure during exfoliation or functionalization. Raman analysis has been used to evaluate oxidation of BP by comparing the A_g^1/A_g^2 ratio, with a value of > 0.6 indicative of the presence of non-oxidized BP.[8,34] The oxide content was assessed using Raman analysis as shown in Table S1 (see Supporting information) with an A^1_g/A^2_g ratio of 0.65 for freshly exfoliated BP. The A^1_g/A^2_g ratio did not change significantly after 1 week of ambient exposure (0.64), however Kuntz *et al.*[33] reported that Raman analysis does not adequately probe the initial stages of oxidation. Photoluminescence (PL) was used to confirm the presence of monolayer BP after exfoliation and functionalization. Figure 1d shows the PL spectrum of exfoliated BP with a broad peak centered at 600 nm associated with monolayer BP.[8] After functionalization with FPI the peak associated with monolayer BP is retained but broadens and shifts to 625 cm^{-1} as a result of induced strain or the electron withdrawing nature of the substituent.[35] Additional PL analysis of MPI and PPI functionalized BP is displayed in Figure S6 which shows a broadening and shift of the peak to 625 cm^{-1} similar to FPI functionalized BP.

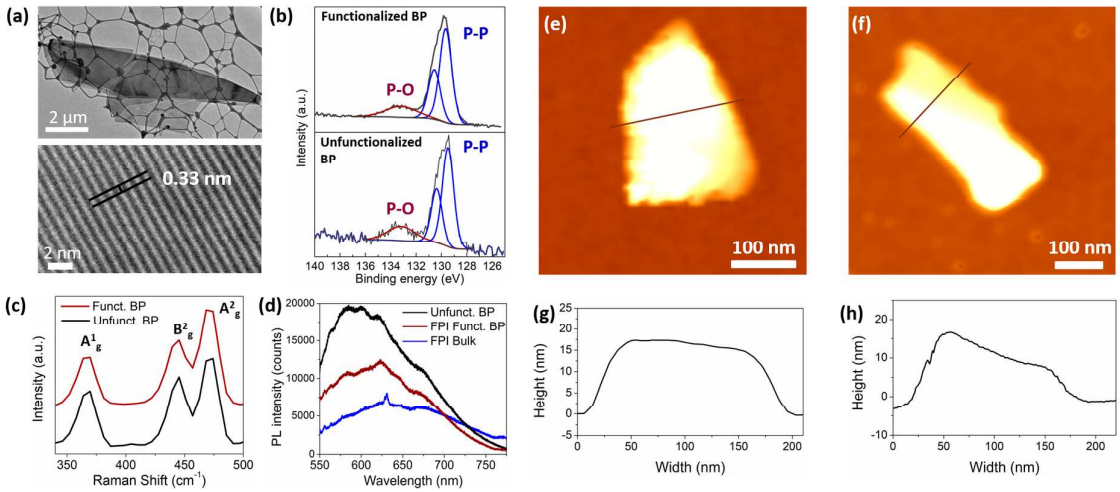

Figure 1. (a) TEM analysis of exfoliated BP. (b) P 2p XPS core level and (c) Raman analysis before (bottom) and after (top) FPI functionalization. (d) PL analysis of exfoliated BP (top), FPI functionalized BP (middle) and bulk FPI (bottom) is displayed. AFM analysis displayed for (e) bare BP and (f) FPI functionalized BP. Height profiles are displayed for (g) bare and (h) functionalized BP.

In addition to the survey spectra, reaction of iodonium salts with BP resulting in covalent modification is further supported by the C1s, F1s and I 3d high resolution spectra. Figure 2a shows the C 1s core level of FPI functionalized BP deconvoluted into 3 components: C-C at 284.5 eV, C-O, C-O-P and C-C-F at 285.5 eV and C-F at 287 eV.[36] The C-P component has been reported at 284 eV,[17] however, this could not be deconvoluted from the C-C peak. Figure 2b shows the absence of a I 3d peak in the core level spectrum indicating reaction of the iodonium moiety with the BP surface resulting in attachment of Ar-F group, which is further supported by the F 1s core level in Figure 2c. The driving force for arylation reactions using iodonium salts is the excellent leaving group ability of the aryl iodide as depicted in the reaction scheme in Figure 2e. An advantage of iodonium salts over diazonium salts is the potential to covalently attach alkyl groups to BP. BP was functionalized using an asymmetrical iodonium salt (perfluoro-n-propyl)phenyliodonium triflate (PPI). Figure 2d shows the F 1s core level after functionalization indicating presence of the fluoroalkyl group.

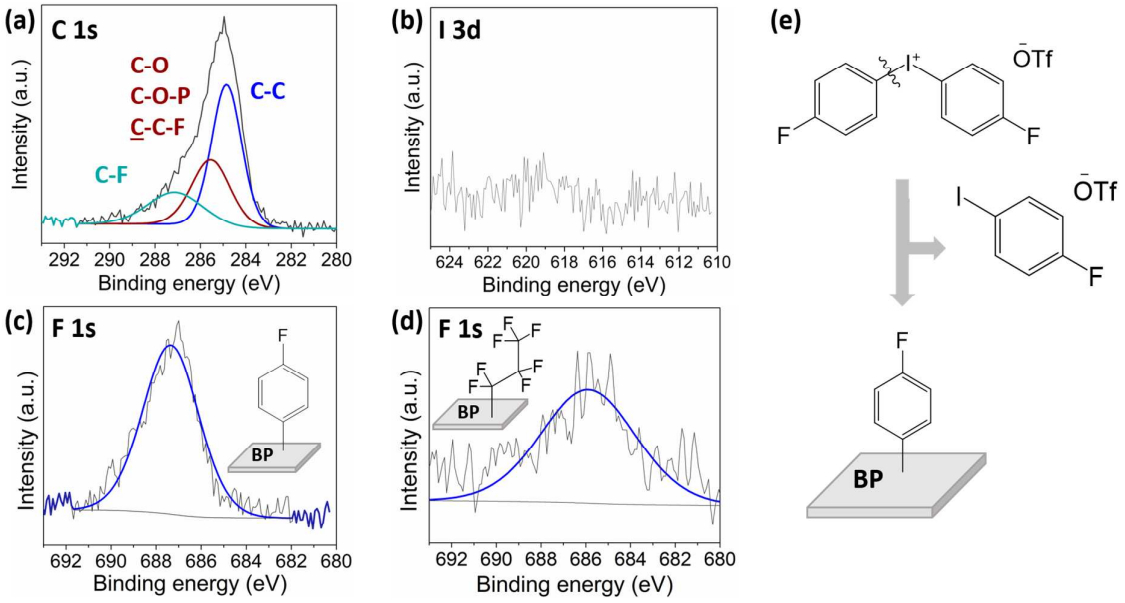

Figure 2: XPS analysis of iodonium functionalized BP. The C 1s displays 3 components due to the presence of C-C at 284.8 eV, C-O, C-O-P and C-C-F at 285.5 eV and C=O and C-F at 287 eV. (b) The I 3d and (c) F 1s core level spectra for FPI functionalized BP and (d) F 1s for PPI functionalized BP. (e) The functionalization using iodonium salts results in the dissociation of the iodonium salt and formation of aryl iodide leaving group resulting in a F-Ar functionalized BP surface

The FTIR spectrum of BP functionalized using FPI displayed in Figure 3a shows the aromatic C-F stretch at 1260 cm^{-1}, aromatic C-H in-plane bend at 1025 cm^{-1}, aromatic C-H out-of-plane bend at 845 cm^{-1} and a marked reduction of the triflate anion at 1163 cm^{-1},[37] all of which indicate aryl functionalization by iodonium salts. The peak at 1186 cm^{-1} may be attributed to P-O-Ar groups possibly indicating attachment of aryl groups to surface oxygen sites, however other P-O peaks are known to occur in this region.[38,39]

Reaction optimization of BP using FPI are detailed in Figure S7 with the optimal conditions giving minimal BP oxidation found to be a 3 h reaction carried out at room temperature. Diaryliodonium salts allow the nature of the ring substituent to be readily changed. Figure 3b

shows the FTIR analysis of BP functionalized with bis(4-methylphenyl)iodonium hexafluorophosphate (MPI). The reduction of the vibrational peaks associated with PF_6^- at 810 cm^{-1} and the remaining aromatic C-H bend at 840 cm^{-1} indicates aryl functionalization of BP (Figure 3b). The FTIR spectra of PPI functionalized BP displayed in Figure 3c, show the C-F stretches observed at 1270 and 1320 cm^{-1} for the bulk salt shifted to 1260 and 1316 cm^{-1} in the PPI functionalized spectrum. Presence of absorption peaks associated with the fluorinated alkyl group and the absence of aromatic C-H vibrational frequencies (Figure S8) suggests preferential attachment of the alkyl group rather than the phenyl group, which was further confirmed by the F 1s core level (Figure 2d). Electrochemical functionalization of glassy carbon electrodes using asymmetrical iodonium salts also results in attachment of the alkyl group.[40] This chemoselectivity is driven by the excellent leaving group ability of the aryl iodide group. To estimate the extent of functionalization using different iodonium precursors the F 1s:P 2p ratio of the FPI and PPI precursors was evaluated. Accounting for the number of F atoms within the fluoroalkyl chain, XPS indicated the F content to be ~40% lower for the PPI precursor compared to the FPI precursor, suggesting a lower extent of functionalisation using the unsymmetrical salt compared to diaryliodonium salts.

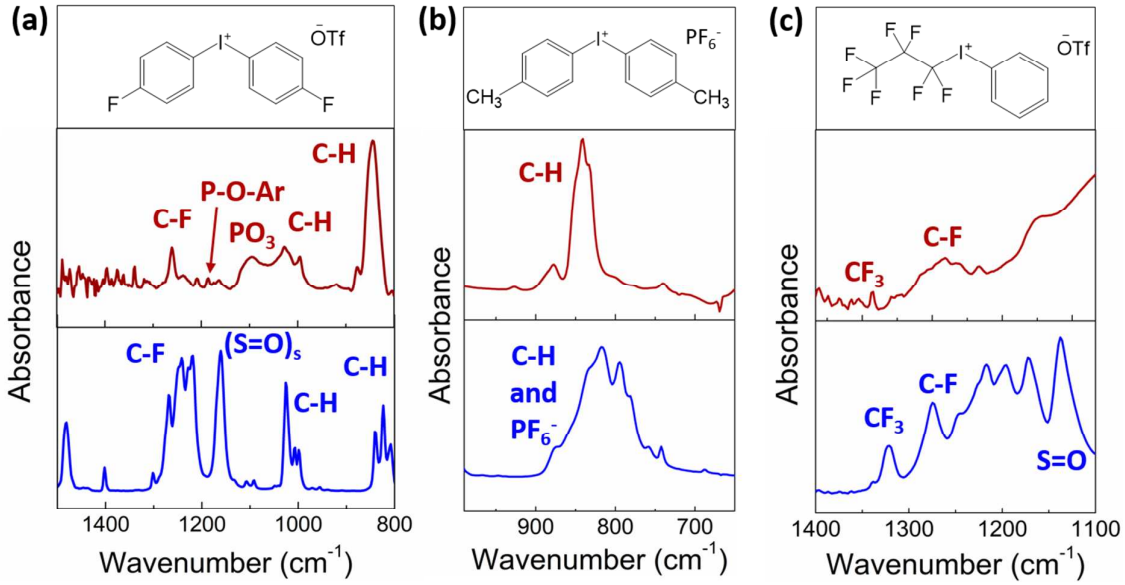

Figure 3. IR analysis of (a) Bis(4-fluorophenyl)iodonium triflate (FPI) (b) Bis(4-methylphenyl)iodonium hexafluorophosphate(MPI) (c) (Perfluoro-n-propyl)phenyliodonium triflate (PPI). The bulk powders are displayed at the bottom (blue) while iodonium functionalized BP is shown at the top (red).

FTIR and XPS analysis were used to confirm successful surface modification of BP using diazonium salts (Figure S4 and S9). IR analysis of BP using aryl diazonium salts, shown in Figure S9, displays the presence of C-H stretches at 860 cm^{-1}, C-F peaks in the 1400-1100 cm^{-1} region and disappearance of the N=N group, indicating successful diazonium modification of BP. The general mechanism of aryl functionalization using diazonium salts has been well studied on carbon, metal and semiconductor surfaces.[41–44] Diazonium salts react with graphene through an electron transfer mechanism from an unpaired electron on the graphene substrate producing aryl radicals. The formation of the reactive aryl radical species is the basis of its reactivity towards pristine BP due the presence of dangling bonds,[17] which is also supported by DFT calculations of BP with NO.[45] DFT calculations show arylation of BP to be thermodynamically favorable but induces significant lattice distortion as phosphorus atoms adopt four-coordinate bonding.[17] However, Sofer *et al.*[19] proposed insertion of the aryl group into P-P bonds with P atoms remaining trivalent. Interestingly, while Ryder et al.[17] reported increased stability using diazonium salts, Sofer *et al.*[19] reported the method to give a low degree of aryl modification and induced BP oxidation. Ryder utilized the diazonium salt in a Bu_4NPF_6 electrolyte-ACN solvent, while Sofer utilized only DMF, which may indicate the extent of functionalization is sensitive to reaction conditions. Diazonium salts can be

hazardous or unstable at room temperature depending on the counterion. In contrast, iodonium salts are non-toxic, air- and moisture stable and therefore a safer and more versatile alternative, widely used in organic synthesis as arylating agents.[20,46] Diaryliodonium salts are effective electrophilic arylating reagents towards a variety of nucleophiles and have been used for *C*-, *O*-, *N*- *S*- and indeed *P*-arylation.[20,22] XPS and IR show reaction of the iodonium group resulting in the presence of Ar-F groups on the BP surface, although the nature of the attachment chemistry is unclear. The ability of diaryliodonium salts to arylate both O and P nucleophiles is a key advantage over diazonium salts where reactivity is only proposed to occur at the P site on BP.[17] Nucleophiles can interact with diaryliodonium salts via different pathways. In the general mechanism for metal-free applications, the nucleophile undergoes a ligand exchange with the counterion and this intermediate then undergoes a ligand coupling, driven by the release of iodobenzene, to form the arylated product.[20] Fearnley *et al.*[25] reported arylation of organic phosphines using diaryliodonium salts to produce aryl-substituted phosphonium salts. The reaction is proposed to proceed via an aryl radical, suggesting arylation of BP may proceed via a similar radical mechanism to diazonium salts giving tetravalent P, which would be positively charged as depicted in Scheme 1a. FTIR analysis in Figure 3a shows the presence of a very minor S=O peak associated with the triflate anion, which is also shifted to a to a higher wavenumber form the bulk salt, indicating the anion might play a role in neutralizing the positive surface charge after the formation of C-P bonds. However, XPS analysis (Figure S10) reveals no significant S 2p peak suggesting that Ar-F groups may attach via O defects. Diaryliodonium salts arylate O nucleophiles including –OH and carboxylic acids.[47,48] Diaryliodonium salts are also effective arylating agents for organophosphorus species such alkyl phosphonates and phosphonic acids. [24,49] Furthermore, Sofer *et. al.*[19] reported that surface oxygen groups react with alkyl halides resulting in the covalent attachment of alkyl groups. Consequently, diaryliodonium salts

which are highly electrophilic, may react through O surface functionalities as depicted in Scheme 1(b) and (c). The attachment chemistry is challenging to evaluate using XPS due to the difficulty in deconvoluting the P-C and P-O-C component in the C 1s and P 2p peaks because of overlap with C-O or P-O components. FTIR analysis shown in Figure 3a indicates the presence of a P-O-C peak, although other P-O peaks can occur in this region. Additionally, the IR spectrum of bare BP (Figure S11) displays an intense peak at 1665 cm^{-1} attributed to the O=P-OH stretch. After functionalization there is the appearance of peaks associated with aromatic C-H bends at 860 cm^{-1} and a significant decrease in the O=P-OH peak intensity which may be associated with reaction of the POH to form P-O-Ar groups, although the exact attachment remains to be elucidated.

Another important surface passivation pathway clearly identified by analysis of the N 1s core level is the passivation role of the reaction solvent. The end product observed for surface modification using both iodonium and diazonium salt is a mixed covalent functionalized BP with the presence of non-covalent passivation by the solvent, ACN, as depicted in Scheme 1(d).

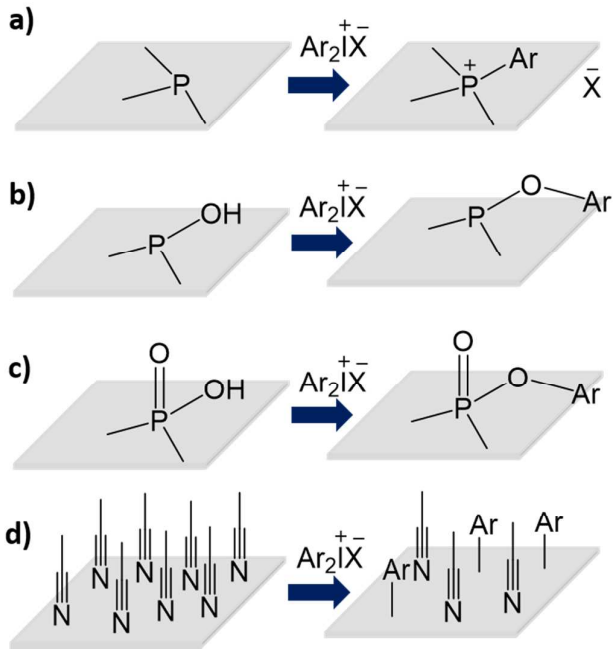

Scheme 1 Aryl functionalization of BP using diaryliodonium salts illustrating arylation through (a) P site, and (b)-(c) O sites. (d) Presence of mixed covalent and non-covalent passivation of the solvent, ACN.

Functionalization using diazonium salts has been reported using mechanically exfoliated BP;[17] however, the N 1s core level and surface chemistry of aryl modified BP were not studied in detail. An advantage of functionalizing liquid exfoliated BP is the facile removal of the solvent compared to residues often transferred to the BP surface after mechanical exfoliation.[50] Figure 4a shows the N 1s core level of liquid exfoliated BP functionalized using nitrobenzenediazonium (NBD). The nitro group at a B.E. of 406 eV indicates successful arylation of BP. The presence of an azo peak at 402 eV is indicative of multilayer formation which occurs when diazonium radicals react with surface bound aryl groups as illustrated in Figure 4b.[37] A N 1s peak associated with the reaction solvent (ACN) is observed at a B.E. of 400 eV, due to the presence of non-covalent passivation of BP by ACN. An important step between exfoliation and functionalization is removal of the solvation shell which will occur as a result of successful functionalization. Residual solvent passivation can be detrimental to device performance and is therefore undesirable when using BP in various applications.[31] Unfunctionalized BP displays a N 1s:P 2p ratio of 0.39 due to passivation of BP with ACN. After functionalization with NBD, the N 1s:P 2p ratio increases by a factor of 2.5 due to three specific contributions: the covalent attachment of the aryl-NO_2 group, the azo group due to multilayer formation, and non-covalent functionalization with ACN, which accounts for 33% of the total increase. In comparison, functionalization with iodonium salts decreases the N 1s:P 2p ratio by ~70% indicating greater displacement of solvent species arising from covalent attachment of aryl groups. The higher degree of covalent

functionalization achieved with iodonium salts may be attributed to the ability of diaryliodonium salt to arylate at P and O sites of BP.[24,47]

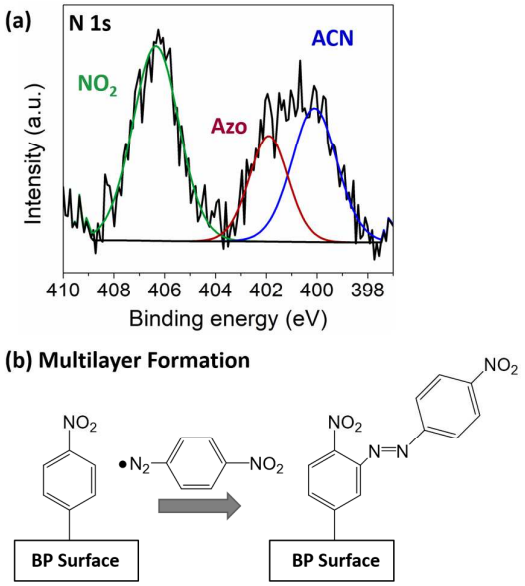

Figure 4. (a) N 1s core level with an azo peak observed at 402 eV. (b) Formation of multilayers through the diazonium radical mechanism

One of the key challenges associated with BP is its limited ambient stability. BP displays a complex oxidation chemistry and literature reports[33,51,52] indicate that both water and oxygen oxidize BP through different mechanisms. Initial oxide formation promotes further oxidation of BP by increasing its hydrophilicity,[33] which has implications for surface functionalization. The greater reactivity of diazonium salts, which proceed via a radical mechanism, always resulted in some degree of BP oxidation, while the lower reactivity of iodonium salts limits oxidation during functionalization. Furthermore, the lack of control when using diazonium

salts, as seen by the presence of multilayers and non-covalent functionalization, are likely to influence stability, as disorder multilayers can give rise to solvent trapping as identified by the N 1s B. E. at 400 eV. The formation of multilayers may also inhibit further covalent functionalization of the BP surface due to steric effects. The impact of aryl functionalization on BP ambient stability was evaluated by comparison to an unfunctionalized BP sample using STEM and XPS analysis. STEM analysis of bare BP after 48 h of ambient exposure (Figure 5 a-b and Figure S12) reveals degradation of crystalline BP with the appearance of topographic protrusions or droplets associated with reaction of BP with ambient water forming H_3PO_4.[32,33,51] STEM analysis of aryl functionalized BP (Figure 5c-d) reveals the crystalline nature is retained after 48 h of ambient exposure. The O 1s and P 2p core levels were used to monitor the oxidation resistance and degradation chemistry of bare and arylated BP. Increased ambient stability of aryl functionalized BP is confirmed by the O 1s and P 2p core level spectra. Deconvolution of the O 1s spectra identified the presence of bridged and non-bridged oxide species on BP. Figure 5e displays the O 1s spectrum of bare BP showing a peak at ~530 eV attributed to the Ti support and a peak at ~532 eV due to non-bridging P oxide species.[51] A minimal amount of bridging oxide species (P-O-P) is displayed at ~535.5 eV[51] indicating minor oxidation as a result of exfoliation, consistent with the P 2p spectrum (Figure 1b). After 40 h of ambient exposure a significant increase in the P-O-P component occurs for bare BP (Figure 5f). Theoretical studies by Ziletti *et al.*[53] reported P-O-P species to be highly unstable and promote BP degradation since bridged oxide species readily form phosphoric acid due to adsorption of water,[54] which correlates with the formation of droplet features observed in STEM analysis. In contrast, aryl functionalized BP showed no increase in the P-O-P component after 40 h as seen in Figure 5g- h. Excellent ambient stability was further confirmed by the P 2p peak with no increase in the P-O shoulder observed after 40 h for aryl modified BP as displayed in Figure 6. The reduction in P-O component observed for

the aryl-BP left in ambient exposure for 40 h is associated with loss of volatile oxides formed by reaction with water. Loss of volatile oxides has been reported to occur in ambient conditions[50,55] and also under vacuum within the XPS chamber.[33,54] The functionalized BP does not undergo further oxidation due to surface passivation however some evaporation of existing oxides occurs and so the oxide component is slightly lower (10.1 %) than the freshly prepared BP (16.3 %). Furthermore, arylation of BP using iodonium salts display superior ambient stability compared to arylation using diazonium salts. After 1 week of ambient exposure the intensity of the oxide peak in the P 2p spectrum increased by 9% (Figure 6c) for aryl functionalized BP using iodonium salts compared to 30% for diazonium salts (Figure S13). The ambient stability of iodonium and diazonium functionalized BP is compared in Figure 6d where the oxide percentage increased more significantly for diazonium functionalized BP. The superior stability of aryl-BP using iodonium salts is attributed to the absence of oxidation during the reaction and greater displacement of ACN solvation shell resulting in covalent attachment of aryl groups.

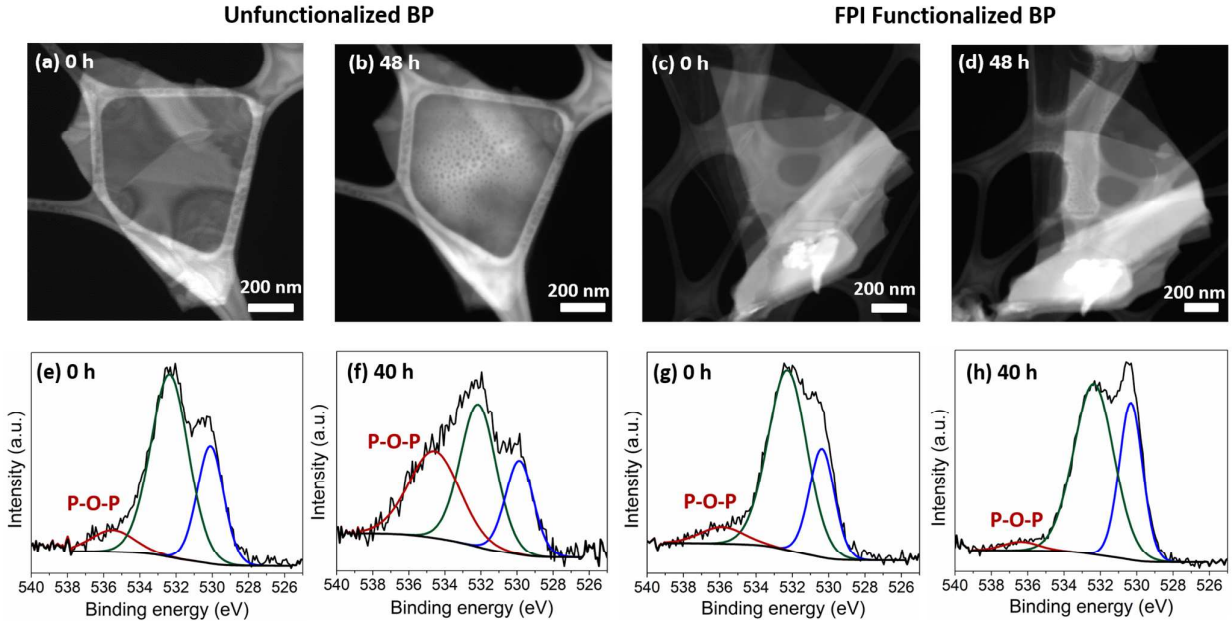

Figure 5. The degradation is analysed using STEM for unfunctionalized BP (a) before and (b) after 48 h of ambient exposure and (c) before and (d) after ambient exposure for FPI functionalized BP. The XPS O 1s peak is displayed (e) before and (f) after 40 h ambient exposure of bare BP and (g) before and (h) after ambient exposure of FPI functionalized BP.

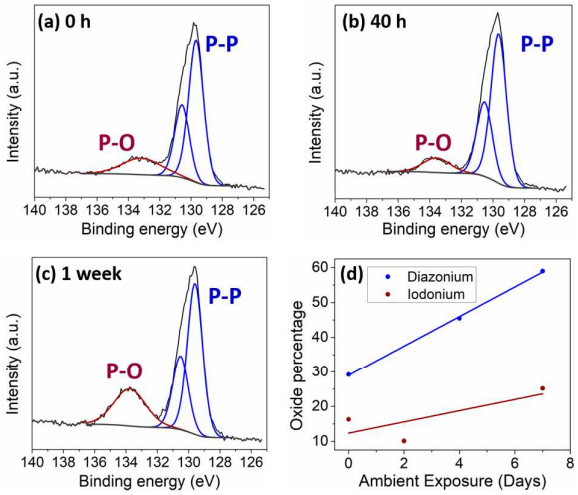

Figure 6. P 2p core levels displaying ambient stability of iodonium functionalized BP over a period of (a) 0 h, (b) 40 h and (c) 1 week. (d) The P 2p oxide percentage is compared for iodonium and diazonium functionalized BP.

Conclusions

We have developed a new method of aryl modification using iodonium salts and demonstrate it as a superior strategy for BP functionalization compared to diazonium salts. Functionalization strategies that have been applied to graphene seem to translate well to BP, however, the puckered honeycomb lattice structure significantly increases its reactivity and lowers its stability. Surface modification using diazonium salts produces mixed covalent and non-covalent functionalization of BP, induces oxidation and the modified BP displays poor ambient stability. The lower reactivity of aryliodonium salts and the ability to possibly arylate both O and P nucleophiles increases its compatibility with BP by enabling covalent functionalization of BP at room temperature with no increase in oxidation. Additionally, aryl modification using iodonium salts limits bridged oxide formation by protecting surface

oxygen sites resulting in excellent ambient stability and potential to tune the electrical properties of BP through covalent attachment of electron donating and withdrawing substituents on the aryl group. Functionalization using iodonium salts can be applied to aryl and alkyl groups providing a new and versatile route to covalent modification of BP which successfully increases its ambient stability.

Author Information

Corresponding Author

*E-mail: g.collins@ucc.ie, Tel: +353 21 420 5143.

Associated Content

Additional characterization of TEM, STEM and SEM analysis, XPS and IR spectra for iodonium and diazonium functionalized BP. This material is available free of charge via the Internet at http://pubs.acs.org.

Acknowledgements

This work was supported by the Irish Research Council Government of Ireland Postgraduate Scholarship Programme under grant number GOIPG/2015/2933 and Science Foundation Ireland (SFI) under grant number 12/RC/2278. This work was also supported by SFI Technology Innovation & Development Award no. 15/TIDA/2893 and under grant no. 14/IA/2581.

References

(1) Liu, H., Neal, A. T., Zhu, Z., Luo, Z., Xu, X., Tománek, D., & Peide, D. Y. Phosphorene : An Unexplored 2D Semiconductor with a High Hole Mobility. *ACS Nano* **2014**, 4, 4033–4041.

(2) Li, L.; Yu, Y.; Ye, G. J.; Ge, Q.; Ou, X.; Wu, H.; Feng, D.; Chen, X. H.; Zhang, Y. Black Phosphorus Field-Effect Transistors. *Nat. Nanotechnol.* **2014**, *9*, 372–377.

(3) Koenig, S. P.; Doganov, R. A.; Schmidt, H.; Castro Neto, A. H.; Özyilmaz, B. Electric Field Effect in Ultrathin Black Phosphorus. *Appl. Phys. Lett.* **2014**, *104*, 103106.

(4) Buscema, M.; Groenendijk, D. J.; Blanter, S. I.; Steele, G. A.; Van Der Zant, H. S. J.; Castellanos-Gomez, A. Fast and Broadband Photoresponse of Few-Layer Black Phosphorus Field-Effect Transistors. *Nano Lett.* **2014**, *14*, 3347–3352.

(5) Gusmao, R.; Sofer, Z.; Pumera, M. Black Phosphorus Rediscovered: From Bulk to Monolayer. *Angew. Chemie Int. Ed.* **2017**, *56*, 8052–8072.

(6) Brent, J. R.; Savjani, N.; Lewis, E. A.; Haigh, S. J.; Lewis, D. J.; O'Brien, P. Production of Few-Layer Phosphorene by Liquid Exfoliation of Black Phosphorus. *Chem Commun.* **2014**, *50*, 13338–13341.

(7) Yasaei, P.; Kumar, B.; Foroozan, T.; Wang, C.; Asadi, M.; Tuschel, D.; Indacochea, J. E.; Klie, R. F.; Salehi-Khojin, A. High-Quality Black Phosphorus Atomic Layers by Liquid-Phase Exfoliation. *Adv. Mater.* **2015**, *27*, 1887–1892.

(8) Hanlon, D.; Backes, C.; Doherty, E.; Cucinotta, C. S.; Berner, N. C.; Boland, C.; Lee, K.; Harvey, A.; Lynch, P.; Gholamvand, Z.; et al. Liquid Exfoliation of Solvent-Stabilized Few-Layer Black Phosphorus for Applications beyond Electronics. *Nat. Commun.* **2015**, *6*, 8563.

(9) Coleman, J. N.; Lotya, M.; O'Neill, A.; Bergin, S. D.; King, P. J.; Khan, U.; Young, K.; Gaucher, A.; De, S.; Smith, R. J.; et al. Two-Dimensional Nanosheets Produced by Liquid Exfoliation of Layered Materials. *Science* **2011**, *331*, 568–571.

(10) Wood, J. D.; Wells, S. A.; Jariwala, D.; Chen, K. S.; Cho, E.; Sangwan, V. K.; Liu, X.;

Lauhon, L. J.; Marks, T. J.; Hersam, M. C. Effective Passivation of Exfoliated Black Phosphorus Transistors against Ambient Degradation. *Nano Lett.* **2014**, *14*, 6964–6970.

(11) Gamage, S.; Fali, A.; Aghamiri, N.; Yang, L.; Ye, P. D.; Abate, Y. Reliable Passivation of Black Phosphorus by Thin Hybrid Coating. *Nanotechnology* **2017**, *28*, 265201.

(12) Lv, W.; Yang, B.; Wang, B.; Wan, W.; Ge, Y.; Yang, R.; Hao, C.; Xiang, J.; Zhang, B.; Zeng, Z.; et al. Sulfur-Doped Black Phosphorus Field-Effect Transistors with Enhanced Stability. *ACS Appl. Mater. Interfaces* **2018**, *10*, 9663–9668.

(13) Yang, B.; Wan, B.; Zhou, Q.; Wang, Y.; Hu, W.; Lv, W.; Chen, Q.; Zeng, Z.; Wen, F.; Xiang, J.; et al. Te-Doped Black Phosphorus Field-Effect Transistors. *Adv. Mater.* **2016**, *28*, 9408–9415.

(14) Xing, C.; Jing, G.; Liang, X.; Qiu, M.; Li, Z.; Cao, R.; Li, X.; Fan, D.; Zhang, H. Graphene Oxide/Black Phosphorus Nanoflake Aerogels with Robust Thermo-Stability and Significantly Enhanced Photothermal Properties in Air. *Nanoscale* **2017**, *9*, 8096–8101.

(15) Sun, J.; Zheng, G.; Lee, H. W.; Liu, N.; Wang, H.; Yao, H.; Yang, W.; Cui, Y. Formation of Stable Phosphorus-Carbon Bond for Enhanced Performance in Black Phosphorus Nanoparticle-Graphite Composite Battery Anodes. *Nano Lett.* **2014**, *14*, 4573–4580.

(16) Cao, Y.; Tian, X.; Gu, J.; Liu, B.; Zhang, B.; Song, S.; Fan, F.; Chen, Y. Covalent Functionalization of Black Phosphorus with Conjugated Polymer for Information Storage. *Angew. Chem. Int. Ed.* **2018**, *57*, 4543–4548.

(17) Ryder, C. R.; Wood, J. D.; Wells, S. A.; Yang, Y.; Jariwala, D.; Marks, T. J.; Schatz, G. C.; Hersam, M. C. Covalent Functionalization and Passivation of Exfoliated Black Phosphorus via Aryl Diazonium Chemistry. *Nat. Chem.* **2016**, *8*, 597–602.

(18) Abellán, G.; Lloret, V.; Mundloch, U.; Marcia, M.; Neiss, C.; Görling, A.; Varela, M.; Hauke, F.; Hirsch, A. Noncovalent Functionalization of Black Phosphorus. *Angew. Chem. Int. Ed.* **2016**, *55*, 14557–14562.

(19) Sofer, Z.; Luxa, J.; Bouša, D.; Sedmidubský, D.; Lazar, P.; Hartman, T.; Hardtdegen, H.; Pumera, M. The Covalent Functionalization of Layered Black Phosphorus. *Angew. Chem. Int. Ed.* **2017**, *56*, 9891–9896.

(20) Merritt, E. A.; Olofsson, B. Diaryliodonium Salts: A Journey from Obscurity to Fame. *Angew. Chem. Int. Ed.* **2009**, *48*, 9052–9070.

(21) Yoshimura, A.; Zhdankin, V. V. Advances in Synthetic Applications of Hypervalent Iodine Compounds. *Chem. Rev.* **2016**, *116*, 3328–3435.

(22) Aradi, K.; Tóth, B. L.; Tolnai, G. L.; Novák, Z. Diaryliodonium Salts in Organic Syntheses: A Useful Compound Class for Novel Arylation Strategies. *Synlett* **2016**, *27*, 1456–1485.

(23) Xu, J.; Zhang, P.; Gao, Y.; Chen, Y.; Tang, G.; Zhao, Y. Copper-Catalyzed P-Arylation via Direct Coupling of Diaryliodonium Salts with Phosphorus Nucleophiles at Room Temperature. *J. Org. Chem.* **2013**, *78*, 8176–8183.

(24) Xiong, B.; Feng, X.; Zhu, L.; Chen, T.; Zhou, Y.; Au, C. T.; Yin, S. F. Direct Aerobic Oxidative Esterification and Arylation of P(O)-OH Compounds with Alcohols and Diaryliodonium Triflates. *ACS Catal.* **2015**, *5*, 537–543.

(25) Fearnley, A. F.; An, J.; Jackson, M.; Lindovska, P.; Denton, R. M. Synthesis of

Quaternary Aryl Phosphonium Salts: Photoredox-Mediated Phosphine Arylation. *Chem. Commun.* **2016**, *52*, 4987–4990.

(26) Vase, K. H.; Holm, A. H.; Norrman, K.; Pedersen, S. U.; Daasbjerg, K. Covalent Graftin of Glassy Carbon Electrodes With Diaryliodomium Salts: New Aspects. *Langmuir* **2007**, *23*, 3786–3793.

(27) He, M.; Swager, T. M. Covalent Functionalization of Carbon Nanomaterials with Iodonium Salts. *Chem. Mater.* **2016**, *28*, 8542–8549.

(28) Chan, C. K.; Beechem, T. E.; Ohta, T.; Brumbach, M. T.; Wheeler, D. R.; Stevenson, K. J. Electrochemically Driven Covalent Functionalization of Graphene from Fluorinated Aryl Iodonium Salts. *J. Phys. Chem. C* **2013**, *117*, 12038–12044.

(29) Koefoed, L.; Pedersen, S. U.; Daasbjerg, K. Covalent Modification of Glassy Carbon Surfaces by Electrochemical Grafting of Aryl Iodides. *Langmuir* **2017**, *33*, 3217–3222.

(30) Brent, J. R.; Savjani, N.; Lewis, E. A.; Haigh, S. J.; Lewis, D. J.; O'Brien, P. Production of Few-Layer Phosphorene by Liquid Exfoliation of Black Phosphorus. *Chem. Commun.* **2014**, *50*, 13338–13341.

(31) Del Rio Castillo, A. E.; Pellegrini, V.; Sun, H.; Buha, J.; Dinh, D. A.; Lago, E.; Ansaldo, A.; Capasso, A.; Manna, L.; Bonaccorso, F. Exfoliation of Few-Layer Black Phosphorus in Low Boiling Point Solvents and Its Application in Li-Ion Batteries. *Chem. Mater.* **2018**, *30*, 506–516.

(32) Yang, T.; Dong, B.; Wang, J.; Zhang, Z.; Guan, J.; Kuntz, K.; Warren, S. C.; Tománek, D. Interpreting Core-Level Spectra of Oxidizing Phosphorene: Theory and Experiment. *Phys. Rev. B - Condens. Matter Mater. Phys.* **2015**, *92*, 125412.

(33) Kuntz, K. L.; Wells, R. A.; Hu, J.; Yang, T.; Dong, B.; Guo, H.; Woomer, A. H.;

Druffel, D. L.; Alabanza, A.; Tománek, D.; et al. Control of Surface and Edge Oxidation on Phosphorene. *ACS Appl. Mater. Interfaces* **2017**, *9*, 9126–9135.

(34) Favron, A.; Gaufrès, E.; Fossard, F.; Phaneuf-L'Heureux, A.-L.; Tang, N. Y.-W.; Lévesque, P. L.; Loiseau, A.; Leonelli, R.; Francoeur, S.; Martel, R. Photooxidation and Quantum Confinement Effects in Exfoliated Black Phosphorus. *Nat. Mater.* **2015**, *14*, 826–832.

(35) Jiang, S.; Krymowski, K.; Asel, T.; Arguilla, M. Q.; Cultrara, N. D.; Yanchenko, E.; Yang, X.; Brillson, L. J.; Windl, W.; Goldberger, J. E. Tailoring the Electronic Structure of Covalently Functionalized Germanane via the Interplay of Ligand Strain and Electronegativity. *Chem. Mater.* **2016**, *28*, 8071–8077.

(36) Robinson, J. T.; Burgess, J. S.; Junkermeier, C. E.; Badescu, S. C.; Reinecke, T. L.; Perkins, F. K.; Zalalutdniov, M. K.; Baldwin, J. W.; Culbertson, J. C.; Sheehan, P. E.; et al. Properties of Fluorinated Graphene Films. *Nano Lett.* **2010**, *10*, 3001–3005.

(37) Collins, G.; Fleming, P.; O'Dwyer, C.; Morris, M. A.; Holmes, J. D.; O'Dwyer, C.; Morris, M. A.; Holmes, J. D. Organic Functionalization of Germanium Nanowires Using Arenediazonium Salts. *Chem. Mater.* **2011**, *23*, 1883–1891.

(38) Bellamy, L. *The Infra-Red Spectra of Complex Molecules*; Springer Science & Business Media, 2013.

(39) Socrates, G. *Infrared and Raman Characteristic Group Frequencies*; John Wiley & Sons, 2001.

(40) Vase, K. H.; Holm, A. H.; Pedersen, S. U.; Daasbjerg, K. Immobilization of Aryl and Alkynyl Groups onto Glassy Carbon Surfaces by Electrochemical Reduction of Iodonium Salts. *Langmuir* **2005**, *21*, 8085–8089.

(41) Bekyarova, E.; Itkis, M. E.; Ramesh, P.; Berger, C.; Sprinkle, M.; De Heer, W. A.; Haddon, R. C. Chemical Modification of Epitaxial Graphene: Spontaneous Grafting of Aryl Groups. *J. Am. Chem. Soc.* **2009**, *131*, 1336–1337.

(42) Paulus, G. L. C.; Wang, Q. H.; Strano, M. S. Covalent Electron Transfer Chemistry of Graphene with Diazonium Salts. *Acc. Chem. Res.* **2013**, *46*, 160–170.

(43) Stewart, M. P.; Maya, F.; Kosynkin, D. V; Dirk, S. M.; Stapleton, J. J.; McGuiness, C. L.; Allara, D. L.; Tour, J. M. Direct Covalent Grafting of Conjugated Molecules onto Si, GaAs, and Pd Surfaces from Aryldiazonium Salts. *J. Am. Chem. Soc.* **2004**, *126*, 370–378.

(44) Lomeda, J. R.; Doyle, C. D.; Kosynkin, D. V.; Hwang, W. F.; Tour, J. M. Diazonium Functionalization of Surfactant-Wrapped Chemically Converted Graphene Sheets. *J. Am. Chem. Soc.* **2008**, *130*, 16201–16206.

(45) Kou, L.; Frauenheim, T.; Chen, C. Phosphorene as a Superior Gas Sensor: Selective Adsorption and Distinct i - V Response. *J. Phys. Chem. Lett.* **2014**, *5*, 2675–2681.

(46) Bonin, H.; Fouquet, E.; Felpin, F. X. Aryl Diazonium versus Iodonium Salts: Preparation, Applications and Mechanisms for the Suzuki-Miyaura Cross-Coupling Reaction. *Adv. Synth. Catal.* **2011**, *353*, 3063–3084.

(47) Jalalian, N.; Petersen, T. B.; Olofsson, B. Metal-Free Arylation of Oxygen Nucleophiles with Diaryliodonium Salts. *Chem. Eur. J.* **2012**, *18*, 14140–14149.

(48) Petersen, T. B.; Khan, R.; Olofsson, B. Metal-Free Synthesis of Aryl Esters from Carboxylic Acids and Diaryliodonium Salts. *Org. Lett.* **2011**, *13*, 3462–3465.

(49) Fañanás-Mastral, M.; Feringa, B. L. Copper-Catalyzed Synthesis of Mixed Alkyl Aryl Phosphonates. *J. Am. Chem. Soc.* **2014**, *136*, 9894–9897.

(50) Island, J. O.; Steele, G. A.; Zant, H. S. J. van der; Castellanos-Gomez, A. Environmental Instability of Few-Layer Black Phosphorus. *2D Mater.* **2015**, *2*, 011002.

(51) Luo, W.; Zemlyanov, D. Y.; Milligan, C. A.; Du, Y.; Yang, L.; Wu, Y.; Ye, P. D. Surface Chemistry of Black Phosphorus under a Controlled Oxidative Environment. *Nanotechnology* **2016**, *27*, 434002.

(52) Huang, Y.; Qiao, J.; He, K.; Bliznakov, S.; Sutter, E.; Chen, X.; Luo, D.; Meng, F.; Su, D.; Decker, J.; et al. Interaction of Black Phosphorus with Oxygen and Water. *Chem. Mater.* **2016**, *28*, 8330–8339.

(53) Ziletti, A.; Carvalho, A.; Campbell, D. K.; Coker, D. F.; Castro Neto, A. H. Oxygen Defects in Phosphorene. *Phys. Rev. Lett.* **2015**, *114*, 26–29.

(54) Edmonds, M. T.; Tadich, A.; Carvalho, A.; Ziletti, A.; O'Donnell, K. M.; Koenig, S. P.; Coker, D. F.; Özyilmaz, B.; Neto, A. H. C.; Fuhrer, M. S. Creating a Stable Oxide at the Surface of Black Phosphorus. *ACS Appl. Mater. Interfaces* **2015**, *7*, 14557–14562.

(55) Castellanos-Gomez, A.; Vicarelli, L.; Prada, E.; Island, J. O.; Narasimha-Acharya, K. L.; Blanter, S. I.; Groenendijk, D. J.; Buscema, M.; Steele, G. a.; Alvarez, J. V.; et al. Isolation and Characterization of Few-Layer Black Phosphorus. *2D Mater.* **2014**, *1*, 025001.

TOC Figure

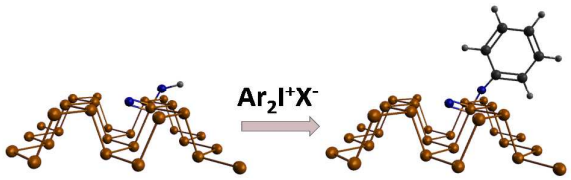
$Ar_2I^+X^-$